7. Negative electrodes in lithium cells (Huggins, ch. 7)

1. Elemental lithium electrodes
2. Problems with the rechargeability of elemental electrodes
3. Lithium-carbon alloys
4. Metallic lithium alloys

Issues

-The use of elemental lithium as the negative electrode → this leads to significant problems

-Negative electrodes currently employed → a solid solution of lithium in one of the forms of carbon

-Lithium cells that operate at temperatures above the melting point of lithium must necessarily use alloys instead of elemental lithium: generally binary or ternary metallic phases

-Increasing current interest in the possibility of the use of metallic alloys instead of carbons at ambient temperatures → the goal of reducing the electrode volume, as well as achieving significantly increased capacity

1. Elemental lithium electrodes

-Elemental lithium has the lowest potential, the lowest weight per unit charge

-Problems with the use of elemental lithium

2. Problems with the rechargeability of elemental electrodes

-Recharging: the electrodeposition of the metal from the electrolyte onto the surface of the electrode → this is not the case → to achieve good rechargeability, a consistent geometry must be maintained on both the macroscopic and the microscopic scales. Both electrical disconnection of the electroactive species and electronic short circuits must also be avoided. In addition, thermal runaway must not occur

(1) Deposition at unwanted locations
(2) Shape change (upon cycling)

(3) Dendrites (수지상)

-Electrode surface local gradient of the element’s chemical potential in the electrolyte adjacent to the solid surface → formation of either dendrites or filaments or nucleation of solid particles

-Dendrites: a tree-and-branches type of morphology

(4) Filamentary growth (섬유상)

-Defects in interface layers: regions of reduced impedance → formation of filamentary growths upon recharge of the electrode → hairy or spongy character → disconnect between metals → capacity↓

(5) Thermal runaway (온도폭증)

-Organic solvent electrolyte are not stable in the presence of high lithium activities → react with lithium and form either crystalline or amorphous product layers → exothermic reaction & local heating (dendrite →surface area↑→thermal runaway)

Alternatives

-Lithium-carbon alloys (current)

-Metallic lithium alloys (R&D): capacity↑

3. Lithium-carbon alloys

-Graphite: graphene layers or sheets → parallel sheets containing interconnected hexagons of carbon → stacking, A-B-A-B-A

-Graphite is amphoteric(양쪽성):

Cations or anions can be Inserted into between Graphene layers

Li^+, K^+, Rb^+…

Br^-, SO_4^{2-}, SbF_6^-…

-1990, Sony: commercialized

-Dependent upon details of Nanostructure & microstructure

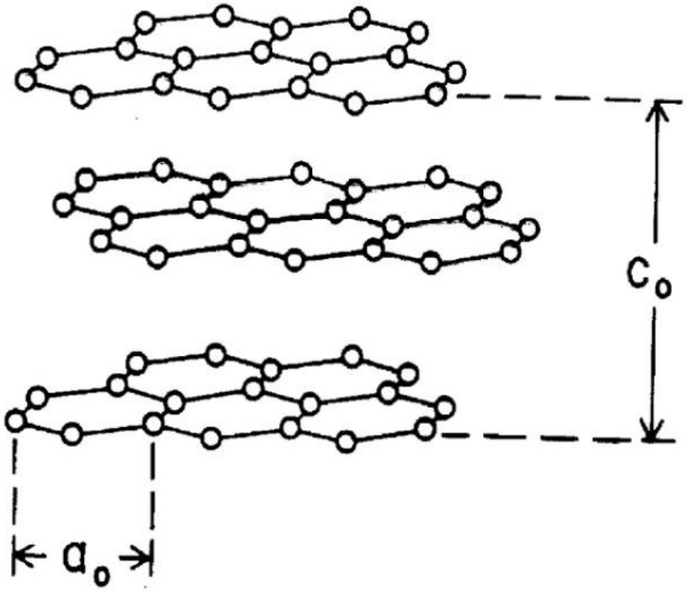

Fig. 7A.1 Model of a portion of the crystal structure of graphite

(1) Ideal structure of graphite saturated with lithium

-Lithium can be inserted into the graphite structure up to a max. of one Li per six carbons, LiC_6 → major in influence of Li in graphite is that the stacking of graphene layers is changed by the insertion of lithium → it changes from A-B-A-B-A stacking to A-A-A-A-A stacking

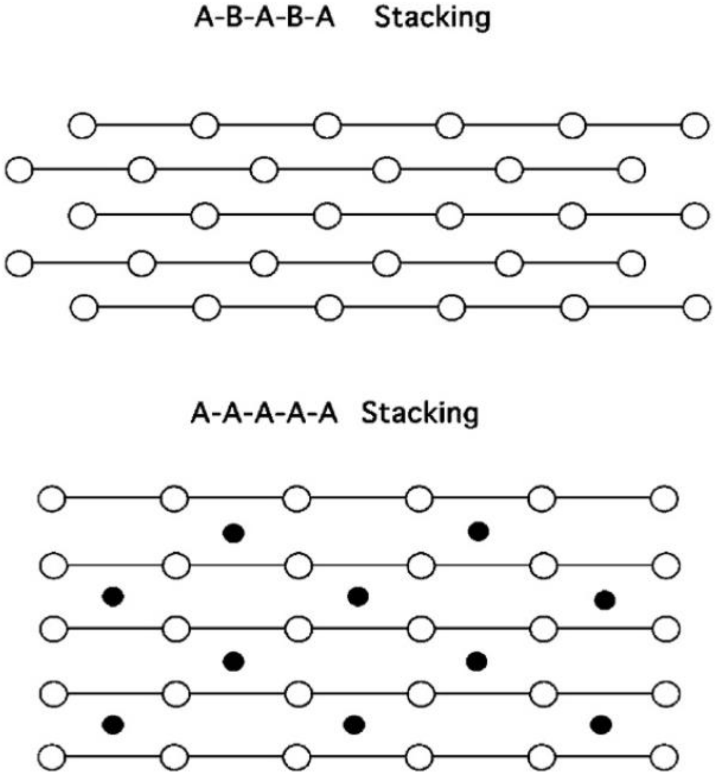

Fig. 7A.2 Difference between the A–B–A–B–A and A–A–A–A–A stacking of the graphene layers when lithium is inserted. The black circles are the lithium ions

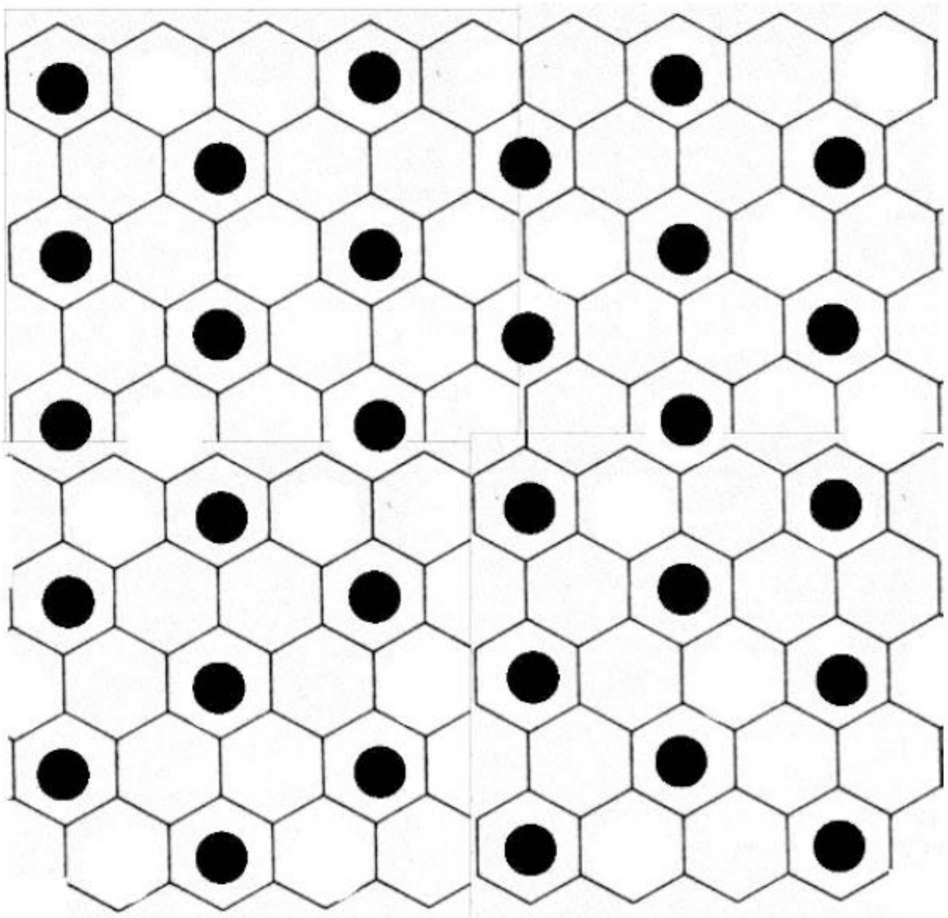

Fig. 7A.3 Schematic representation of the lithium distribution in the gallery space in relation to the carbon hexagonal network in the adjacent graphene layers

(2) Variations in the Structure of Graphite

-lithium–carbon materials do not actually have the ideal graphite structure → closest are made synthetically by vapor transport, called highly ordered pyrolytic graphite (HOPG) → slow and very expensive process → commercially, graphites from natural graphite to materials formed by the pyrolysis of various polymers or hydrocarbon precursors

-two general types: (i) soft, or graphitizing carbons, (ii) hard carbons

(i) *Soft carbons*: produced by the pyrolysis of liquid materials such as petroleum pitch → initially arranged in small graphene-type groups, but imperfection, randomness, disorder → three types of initial disorder (in-plane defects, inter-plane stacking defects, rotational misorientation) gradually become healed as the temperature is raised → at intermediate T, many small 3-D subgrains (Fig. 7A.4)

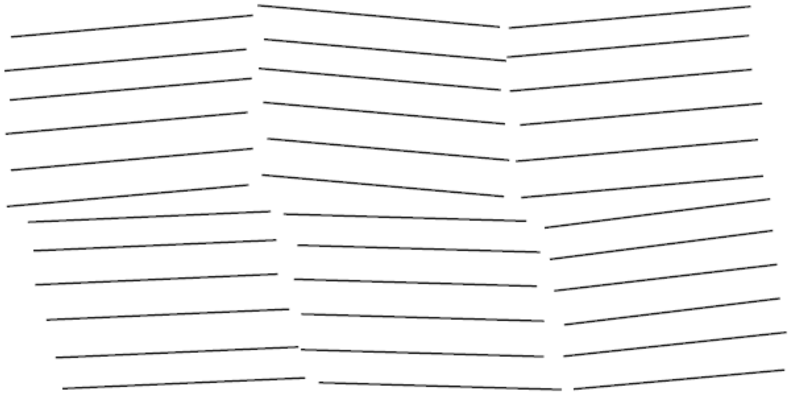

Fig. 7A.4 Schematic drawing of the microstructure of graphite after heating to intermediate temperatures

(ii) *hard carbons*: produced by the pyrolysis of solid materials, such as chars or glassy carbon → initially have a significant amount of initial cross-linking and nanoporosity → As a result, it is more difficult to make these structural rearrangements and turbostratic disorder is more persistent → more thermal energy, i.e., higher temperatures → heating to the range of 1,000–2,000°C produces microstructures in which graphene sheets form and begin to grow, with diameters up to about 15 nm, and small stacks of 50–100 sheets → larger ordered, i.e., graphitic regions from 2,000 to 3,000°C

(3) Structural Aspects of Lithium Insertion into Graphitic Carbons

-Li → C staging? Li that enters the graphite structure is not distributed uniformly between all the graphene layers at ambient temperatures. Instead, it resides in certain interlayer *galleries*, but not others, depending upon the total amount of lithium present

→ The distribution is described by the number of graphene layers between those that have the lithium guest ions present. A stage 1 structure has lithium between all of the graphene layers; a stage 2 structure has an empty gallery between each occupied gallery, and a stage 4 structure has four graphene layers between each gallery containing lithium

→ The phenomenon can be attributed to a catalytic effect, in which the ions that initially enter a gallery pry open the van der Waals-bonded interlayer space, making it easier for following ions to enter

(4) Electrochemical behavior of lithium in graphite

→ highly variable, depending upon the details of the graphitic structure
→ Materials with a more perfect graphitic structure react with lithium at more negative potentials, whereas those with less well organized structures typically operate over much wider potential ranges, resulting in cell voltages that are both lower and more state-of-charge dependent
-commercial batteries: heated to temperatures over about 2,400°C, where they become quite well graphitized. Capacities typically range from 300 to 350mAh g^{-1} (maximum theoretical value (for LiC_6) is **372mAh g^{-1}**)

A typical discharge curve under operating conditions, with currents as large as 2–4mA cm^{-2}, is shown in Fig. 7A.5. This behavior is not far from what is found under near-equilibrium conditions, as shown in Fig. 7A.6

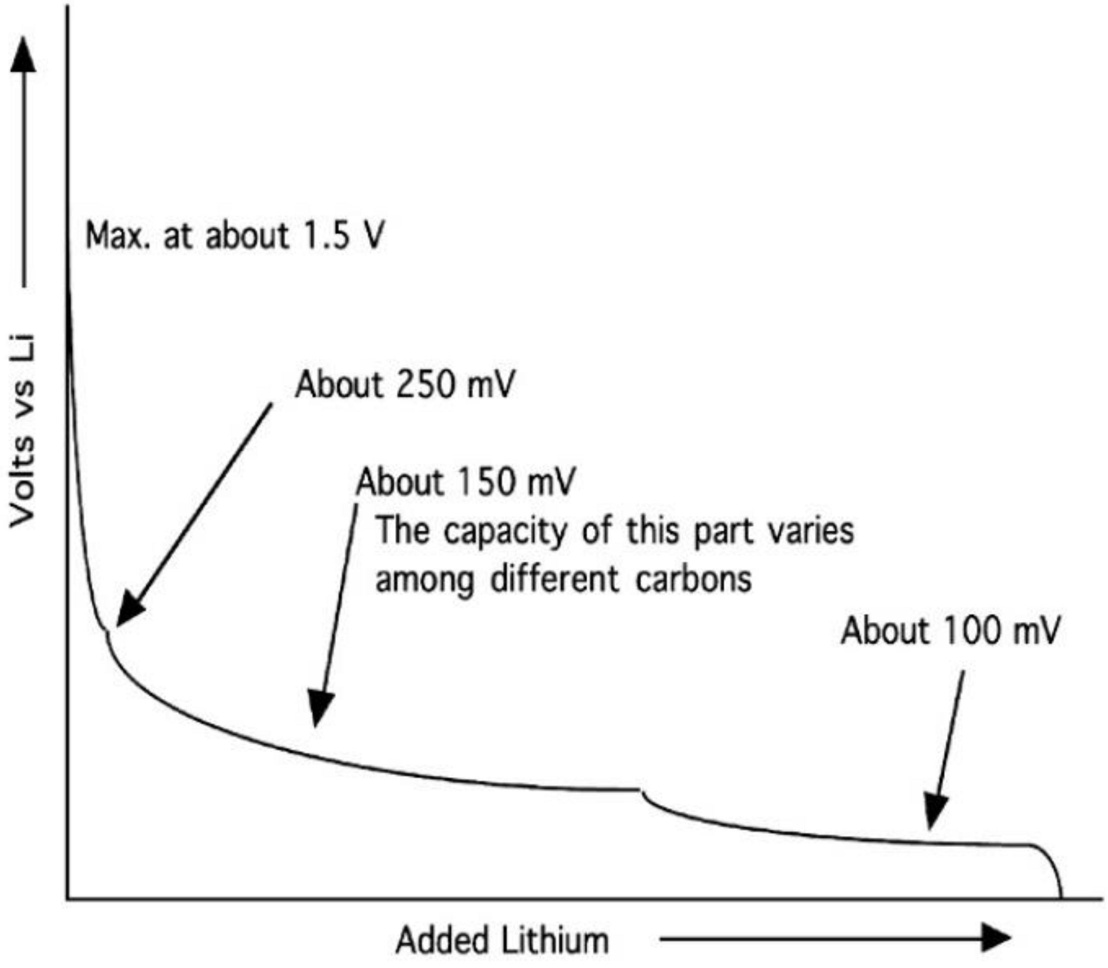

Fig. 7A.5 Typical discharge curve of a lithium battery negative electrode

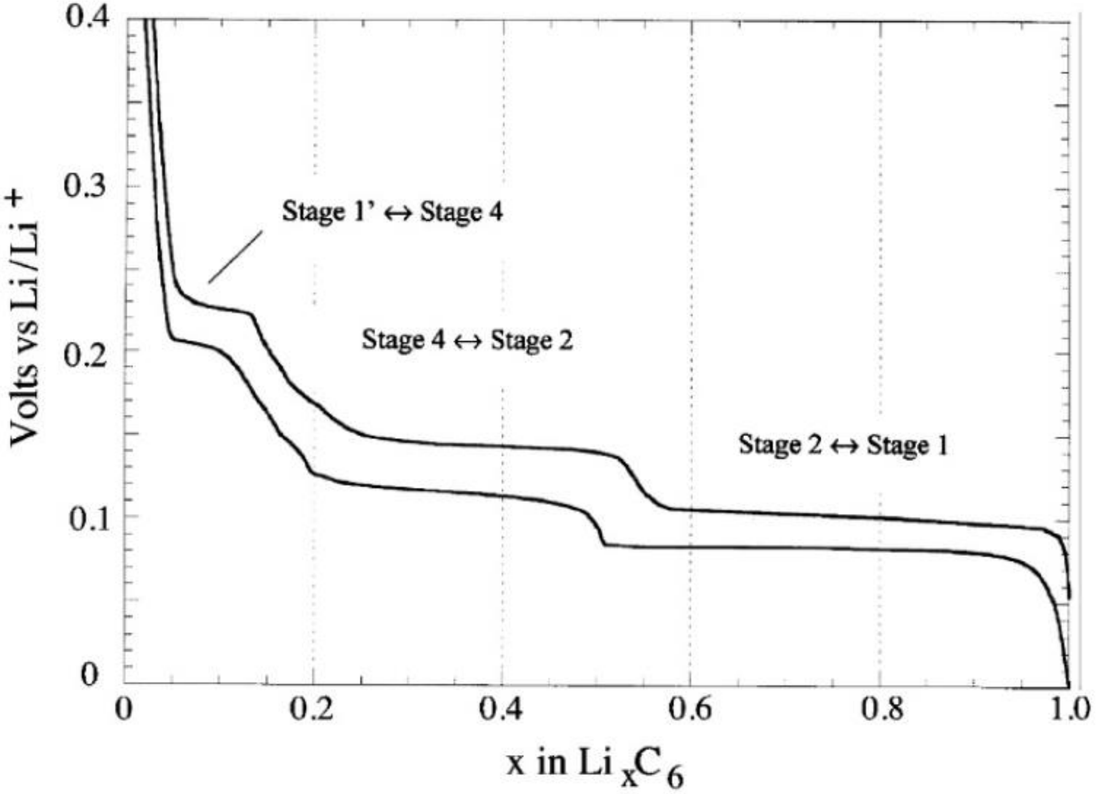

Fig. 7A.6 Potential vs. composition during lithiation and delithiation of a graphite electrode at the C/50 rate at ambient temperature (R. Yazami, personal communication)

(5) Electrochemical Behavior of Lithium in Amorphous Graphite

-electrochemical behavior is quite different when the carbon has not been heated so high, and the structure is not so well ordered → a wide range of possible sites in which the lithium can reside, with different local structures, and therefore different energies → the result that the potential varies gradually, rather than showing the steps characteristic of more ordered structures. This is shown in Fig. 7A.7 → varying with the state of charge, the potential is significantly greater than is found in the graphitic materials → This means that the cell voltages are correspondingly lower

-capacity loss on the first cycle. The capacity upon the first charging (that is not useful) was greater than the capacity in the subsequent discharge cycle. The source of this phenomenon is not yet understood, but there must be some lithium that is *trapped* in the structure

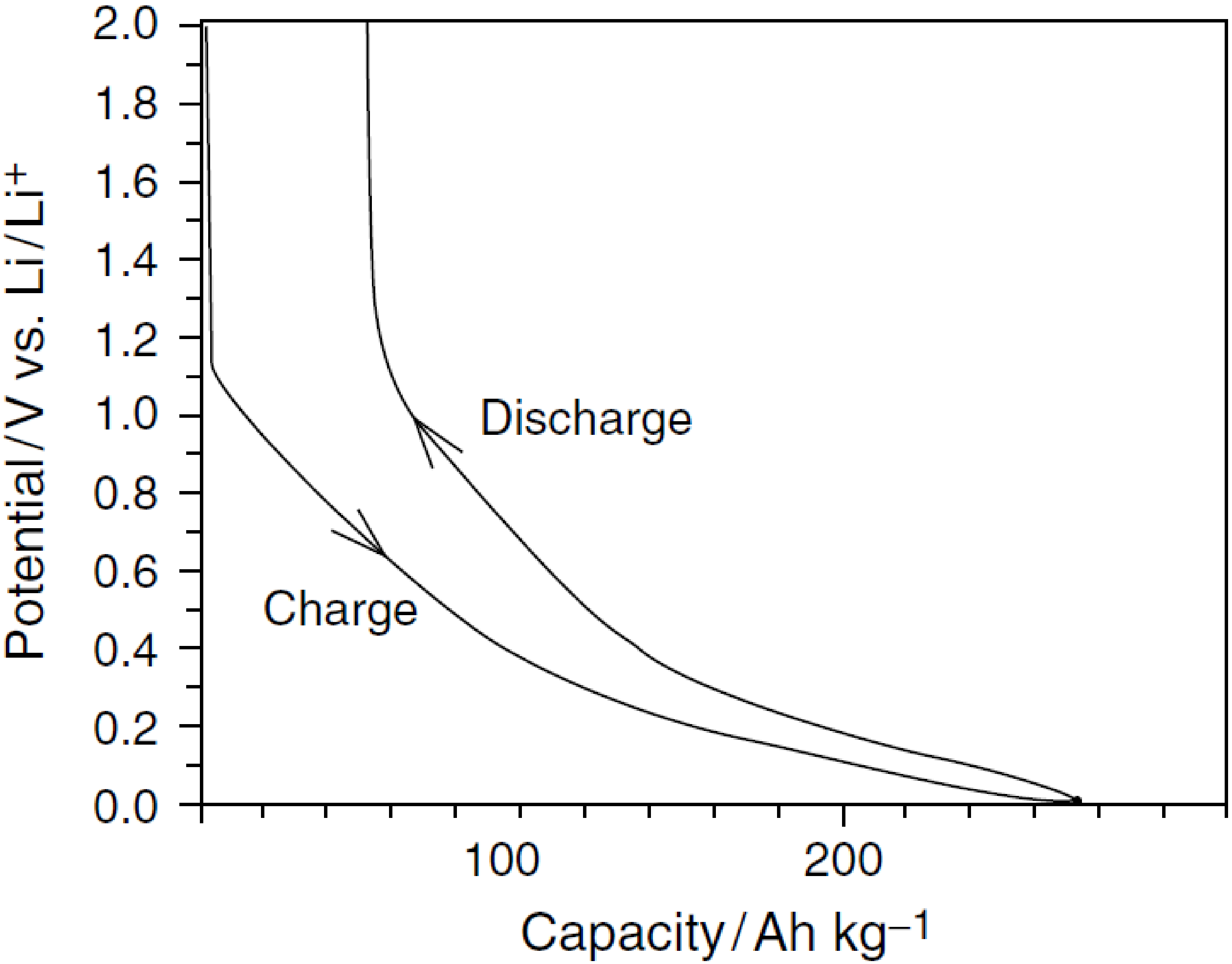

Fig. 7A.7 Typical data for the reaction of lithium with an amorphous carbon [6]

(6) Lithium in Hydrogen-Containing Carbons

-It is often found that there is a considerable amount of hydrogen initially present in various carbons, depending upon the nature of the precursor. This gradually disappears as the temperature is raised

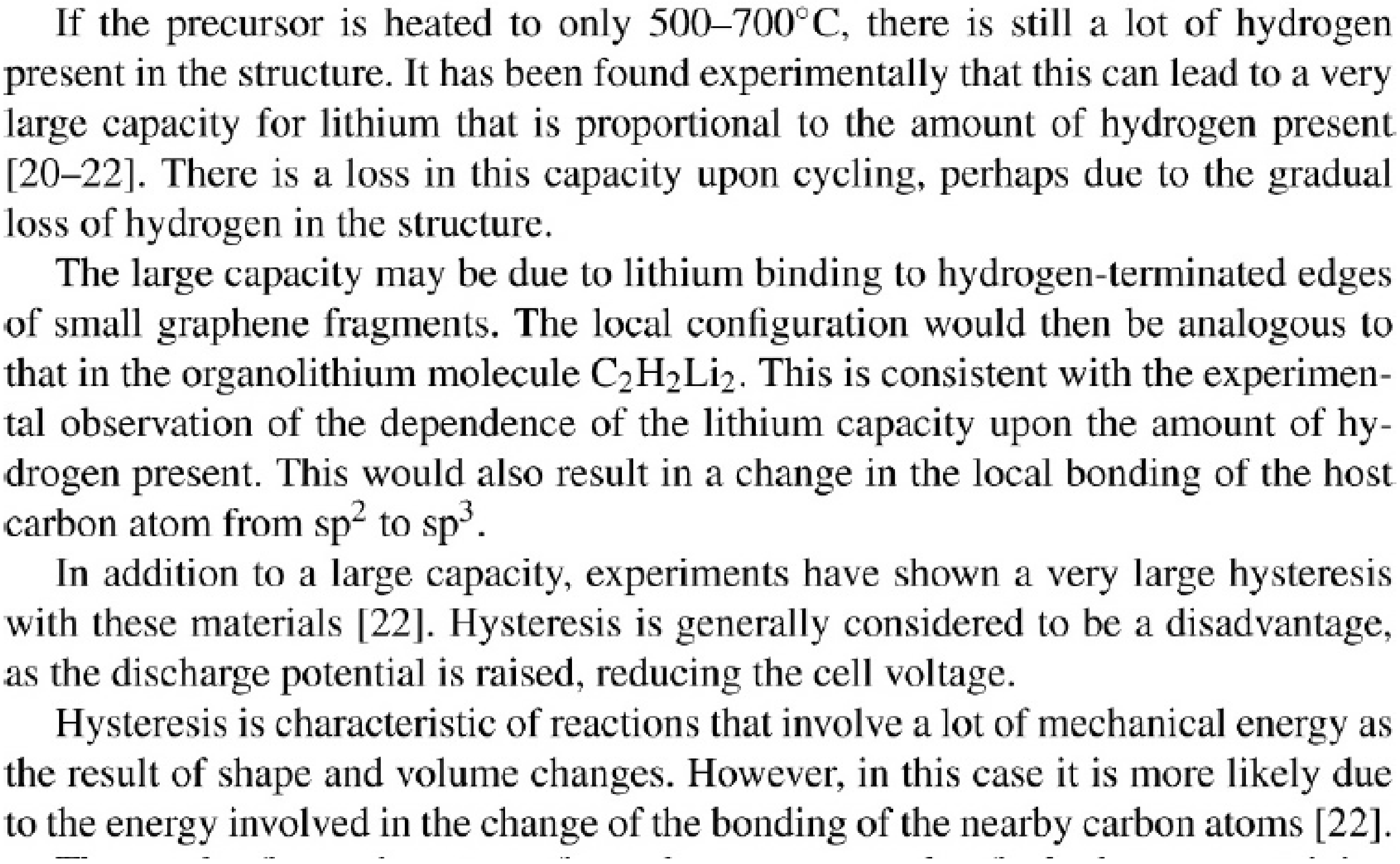

If the precursor is heated to only 500–700°C, there is still a lot of hydrogen present in the structure. It has been found experimentally that this can lead to a very large capacity for lithium that is proportional to the amount of hydrogen present [20–22]. There is a loss in this capacity upon cycling, perhaps due to the gradual loss of hydrogen in the structure.

The large capacity may be due to lithium binding to hydrogen-terminated edges of small graphene fragments. The local configuration would then be analogous to that in the organolithium molecule $C_2H_2Li_2$. This is consistent with the experimental observation of the dependence of the lithium capacity upon the amount of hydrogen present. This would also result in a change in the local bonding of the host carbon atom from sp^2 to sp^3.

In addition to a large capacity, experiments have shown a very large hysteresis with these materials [22]. Hysteresis is generally considered to be a disadvantage, as the discharge potential is raised, reducing the cell voltage.

Hysteresis is characteristic of reactions that involve a lot of mechanical energy as the result of shape and volume changes. However, in this case it is more likely due to the energy involved in the change of the bonding of the nearby carbon atoms [22].

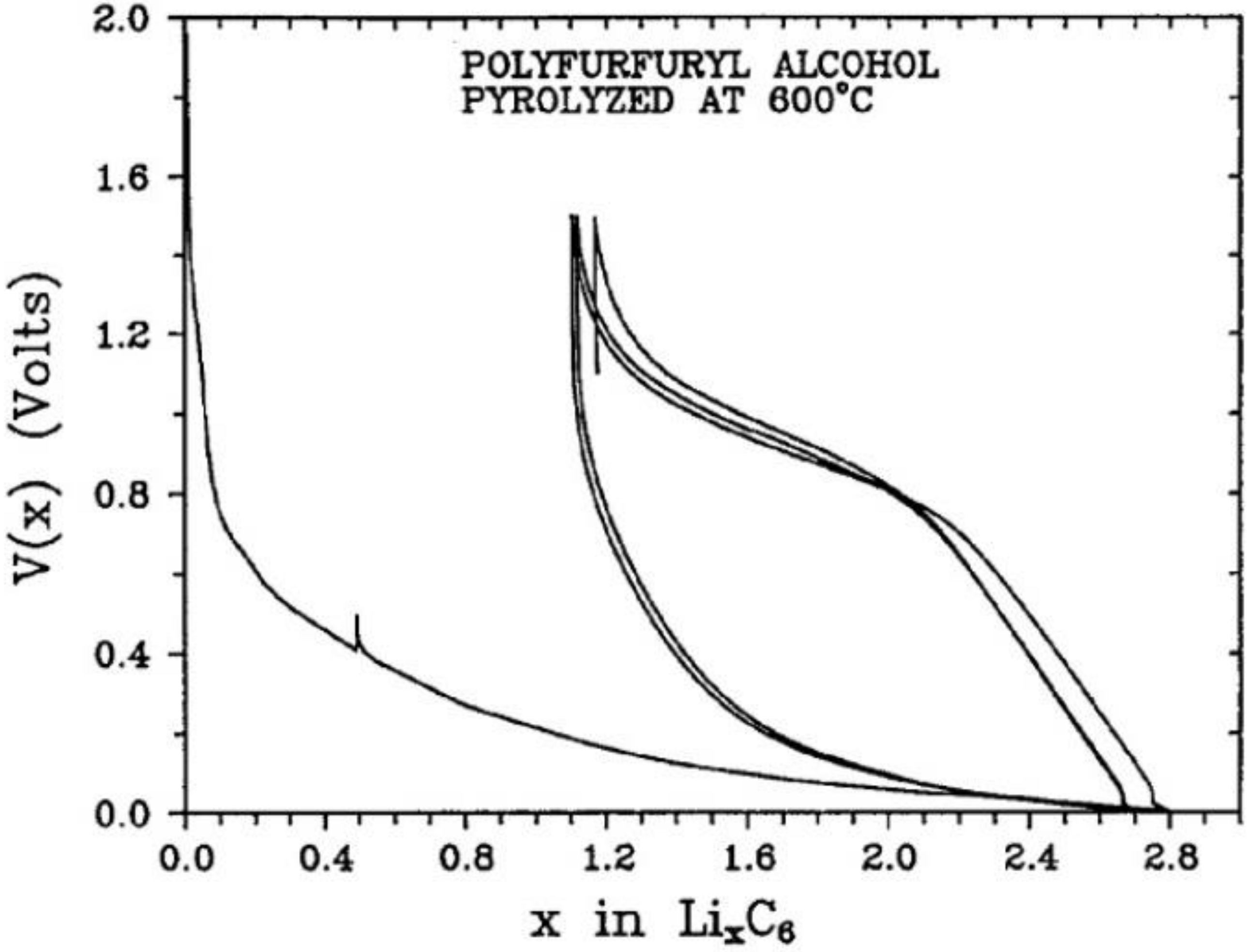

Fig. 7A.8 Charge–discharge curves for a material containing hydrogen [7]

4. Metallic lithium alloys

-Lithium alloys as an alternative to elemental lithium with molten salt electrolytes at 400–450°C (well above the melting point of lithium) were interested in this possibility

-two major directions: Li–aluminum alloys, Li–Si alloys (advantage: can avoid the problems related to lithium melting, two disadvantage: (i) because they reduce the activity of the lithium they necessarily reduce the cell voltage, (ii) the presence of additional species that are not directly involved in the electrochemical reaction always brings additional weight,

and often, volume. Thus the maximum theoretical values of the specific energy are always reduced compared with what might be attained with pure lithium

e.g. thermal battery: Li alloy/FeS_2 in chloride molten salt electrolyte (Li-Si or Li-Al alloys)

(1) Equilibrium thermodynamic properties of binary lithium alloys

-phase diagram and equilibrium thermodynamic properties (LiCl-KCl molten salt electrolyte)

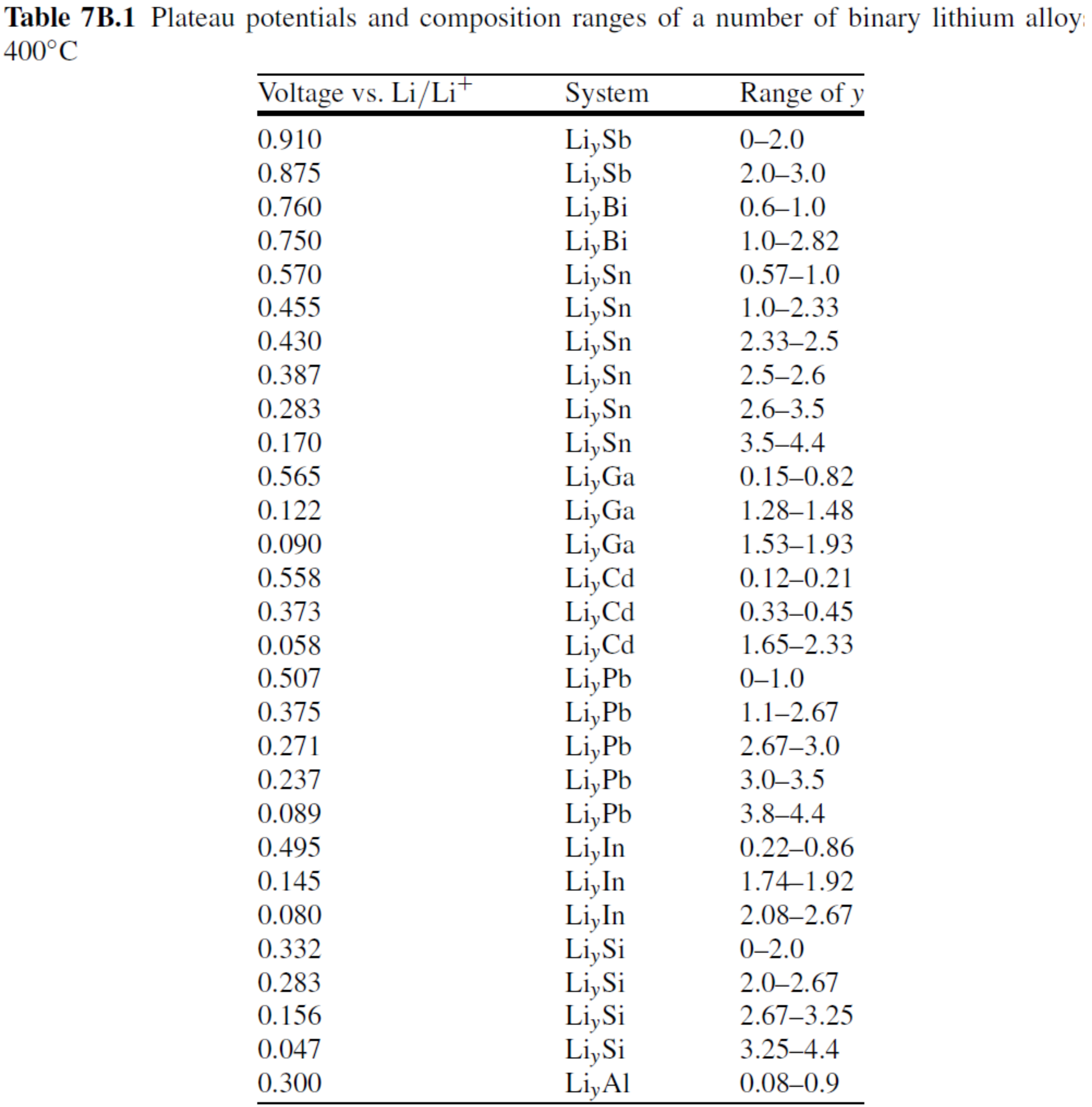

Table 7B.1 Plateau potentials and composition ranges of a number of binary lithium alloy
400°C

Voltage vs. Li/Li$^+$	System	Range of y
0.910	Li_ySb	0–2.0
0.875	Li_ySb	2.0–3.0
0.760	Li_yBi	0.6–1.0
0.750	Li_yBi	1.0–2.82
0.570	Li_ySn	0.57–1.0
0.455	Li_ySn	1.0–2.33
0.430	Li_ySn	2.33–2.5
0.387	Li_ySn	2.5–2.6
0.283	Li_ySn	2.6–3.5
0.170	Li_ySn	3.5–4.4
0.565	Li_yGa	0.15–0.82
0.122	Li_yGa	1.28–1.48
0.090	Li_yGa	1.53–1.93
0.558	Li_yCd	0.12–0.21
0.373	Li_yCd	0.33–0.45
0.058	Li_yCd	1.65–2.33
0.507	Li_yPb	0–1.0
0.375	Li_yPb	1.1–2.67
0.271	Li_yPb	2.67–3.0
0.237	Li_yPb	3.0–3.5
0.089	Li_yPb	3.8–4.4
0.495	Li_yIn	0.22–0.86
0.145	Li_yIn	1.74–1.92
0.080	Li_yIn	2.08–2.67
0.332	Li_ySi	0–2.0
0.283	Li_ySi	2.0–2.67
0.156	Li_ySi	2.67–3.25
0.047	Li_ySi	3.25–4.4
0.300	Li_yAl	0.08–0.9

(2) Experiments at ambient T

-slow kinetics at lower T

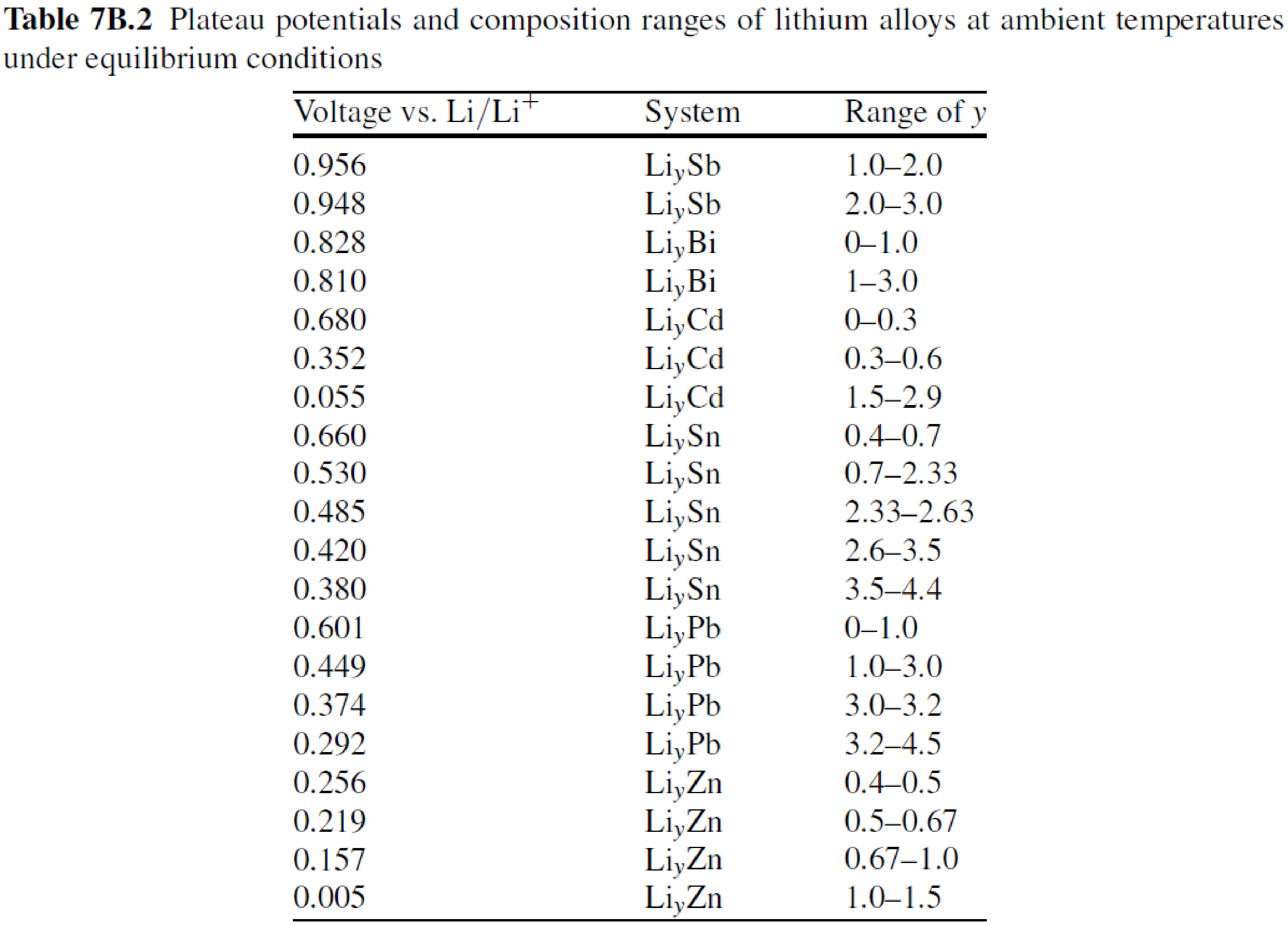

Table 7B.2 Plateau potentials and composition ranges of lithium alloys at ambient temperatures under equilibrium conditions

Voltage vs. Li/Li$^+$	System	Range of *y*
0.956	Li_ySb	1.0–2.0
0.948	Li_ySb	2.0–3.0
0.828	Li_yBi	0–1.0
0.810	Li_yBi	1–3.0
0.680	Li_yCd	0–0.3
0.352	Li_yCd	0.3–0.6
0.055	Li_yCd	1.5–2.9
0.660	Li_ySn	0.4–0.7
0.530	Li_ySn	0.7–2.33
0.485	Li_ySn	2.33–2.63
0.420	Li_ySn	2.6–3.5
0.380	Li_ySn	3.5–4.4
0.601	Li_yPb	0–1.0
0.449	Li_yPb	1.0–3.0
0.374	Li_yPb	3.0–3.2
0.292	Li_yPb	3.2–4.5
0.256	Li_yZn	0.4–0.5
0.219	Li_yZn	0.5–0.67
0.157	Li_yZn	0.67–1.0
0.005	Li_yZn	1.0–1.5

(3) Mixed-conductor matrix electrodes

-electronic conducting matrix for active electrode material

e.g. $Li_{13}Sn_5$ matrix + Li-Si near 400°C → high chemical diffusion coeff. of lithium in $Li_{13}Sn_5$ phase

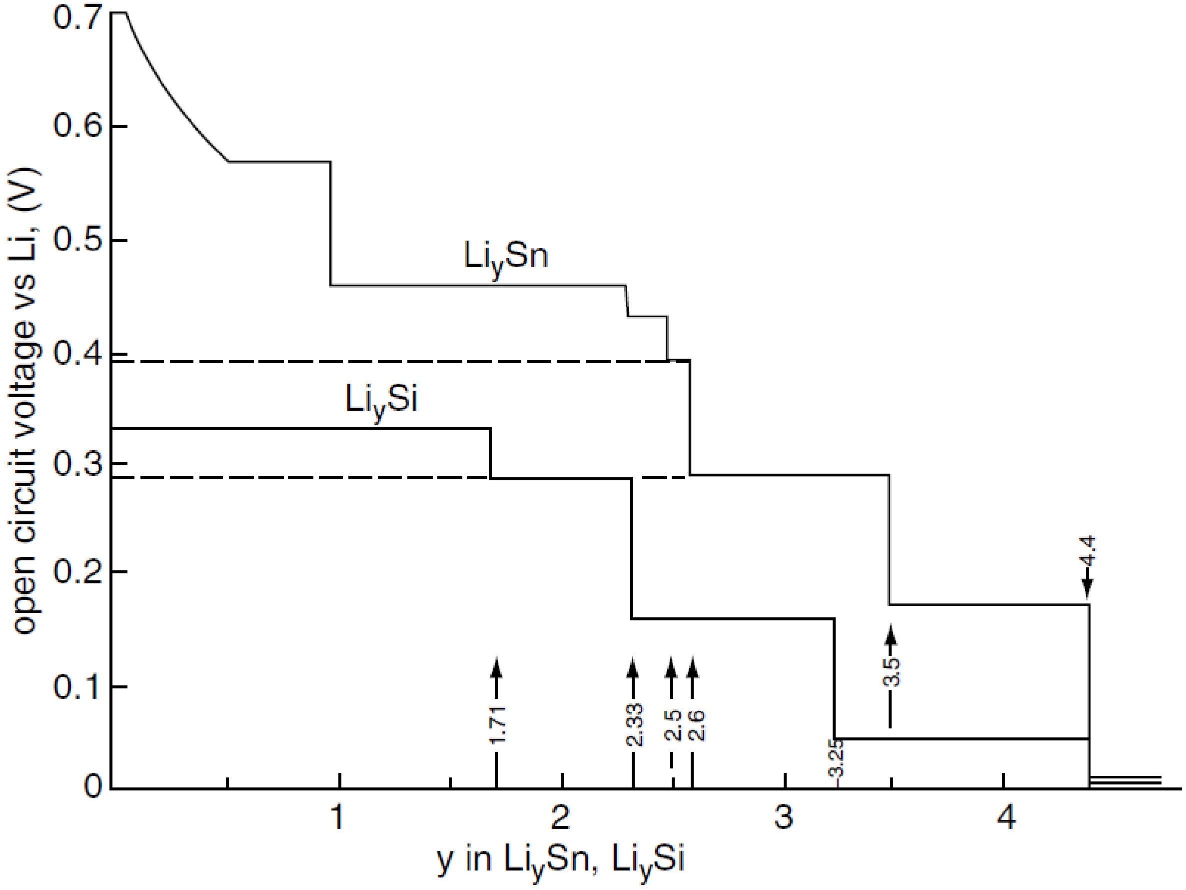

Fig. 7B.1 Composition dependence of the potential in the Li–Sn and Li–Si systems

Fig. 7B.1. $Li_{2.6}Sn(Li_{13}Sn_5)$ is stable over a potential range that includes the upper two-phase reconstitution reaction plateau in the lithium–silicon system. Therefore, lithium can react with Si to form the phase $Li_{1.71}Si$ ($Li_{12}Si_7$) inside an all-solid composite electrode containing the $Li_{2.6}Sn$ phase, which acts as a lithium-transporting, but electrochemically inert matrix

Figure 7B.2 shows the relatively small polarization that is observed during the charge and discharge of this electrode, even at relatively high current densities → a potential overshoot due to the free energy involved in the nucleation of a new second phase if the reaction goes to completion in each direction. On the other hand, if the composition is not driven quite so far, so that there is some of the reactant phase remaining, this nucleation-related potential overshoot does not appear, as seen in Fig. 7B.3

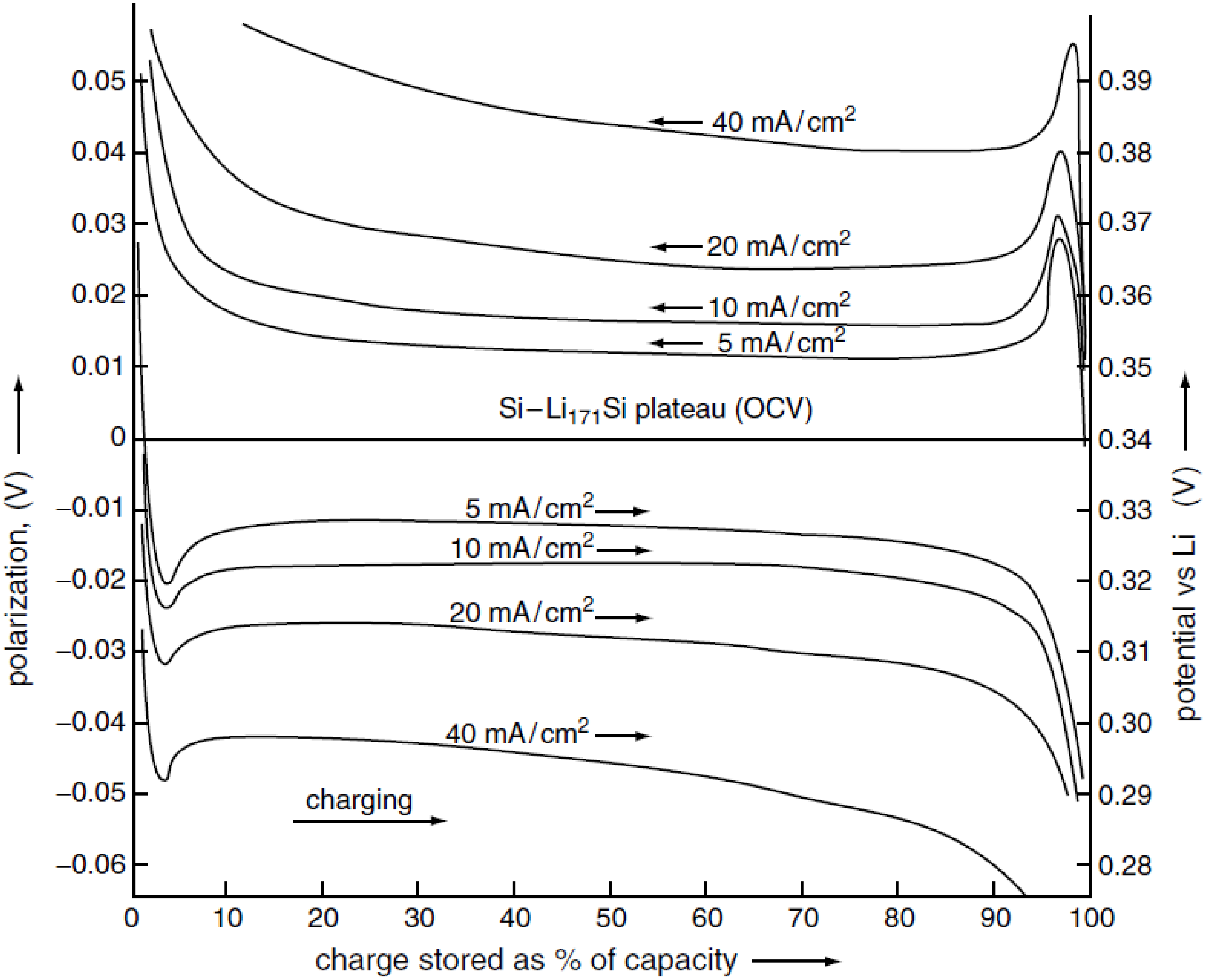

Fig. 7B.2 Charge and discharge curves of the Li–Si alloy in the matrix of the electrochemically inert mixed-conducting Li–Sn alloy at different current densities

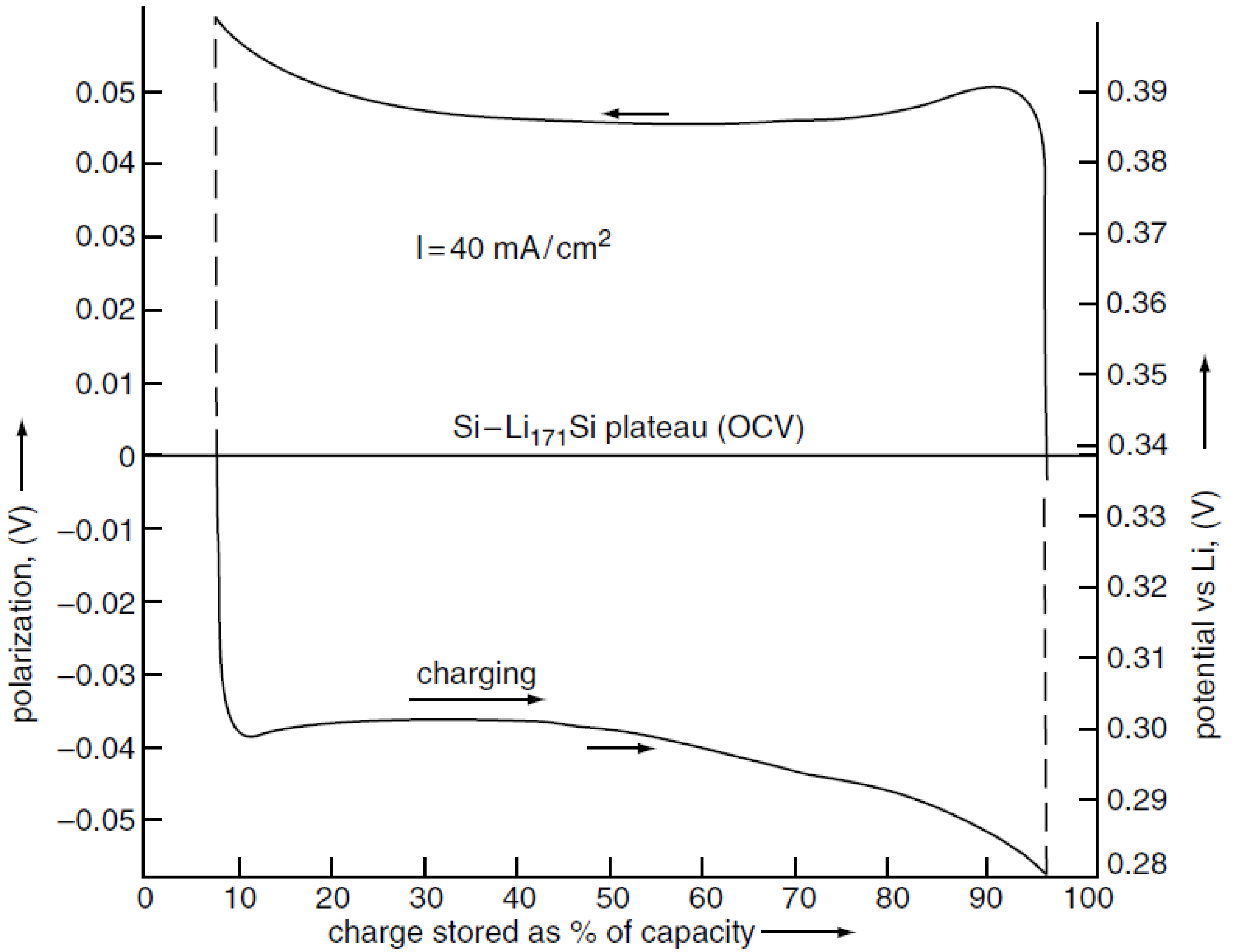

Fig. 7B.3 Charge and discharge curves of the Li–Si, Li–Sn composite if the capacity is limited so that the reaction does not go to completion in either direction. There is no large nucleation overshoot in this case

Li–Sn–Cd system at ambient T

The composition dependence of the potentials in the two binary systems at ambient temperatures

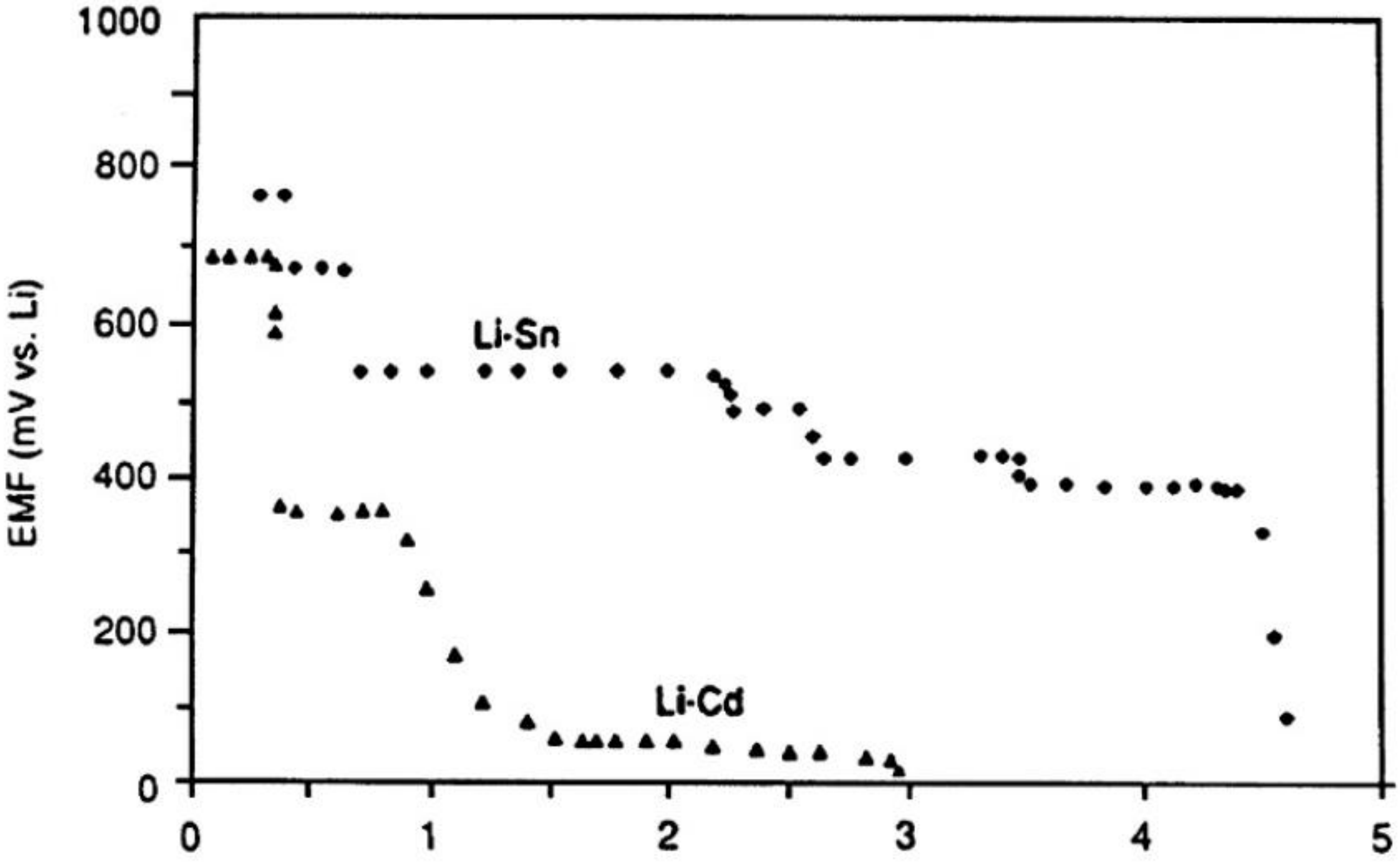

Fig. 7B.4 Potential vs. composition for Li–Sn and Li–Cd systems at ambient temperature

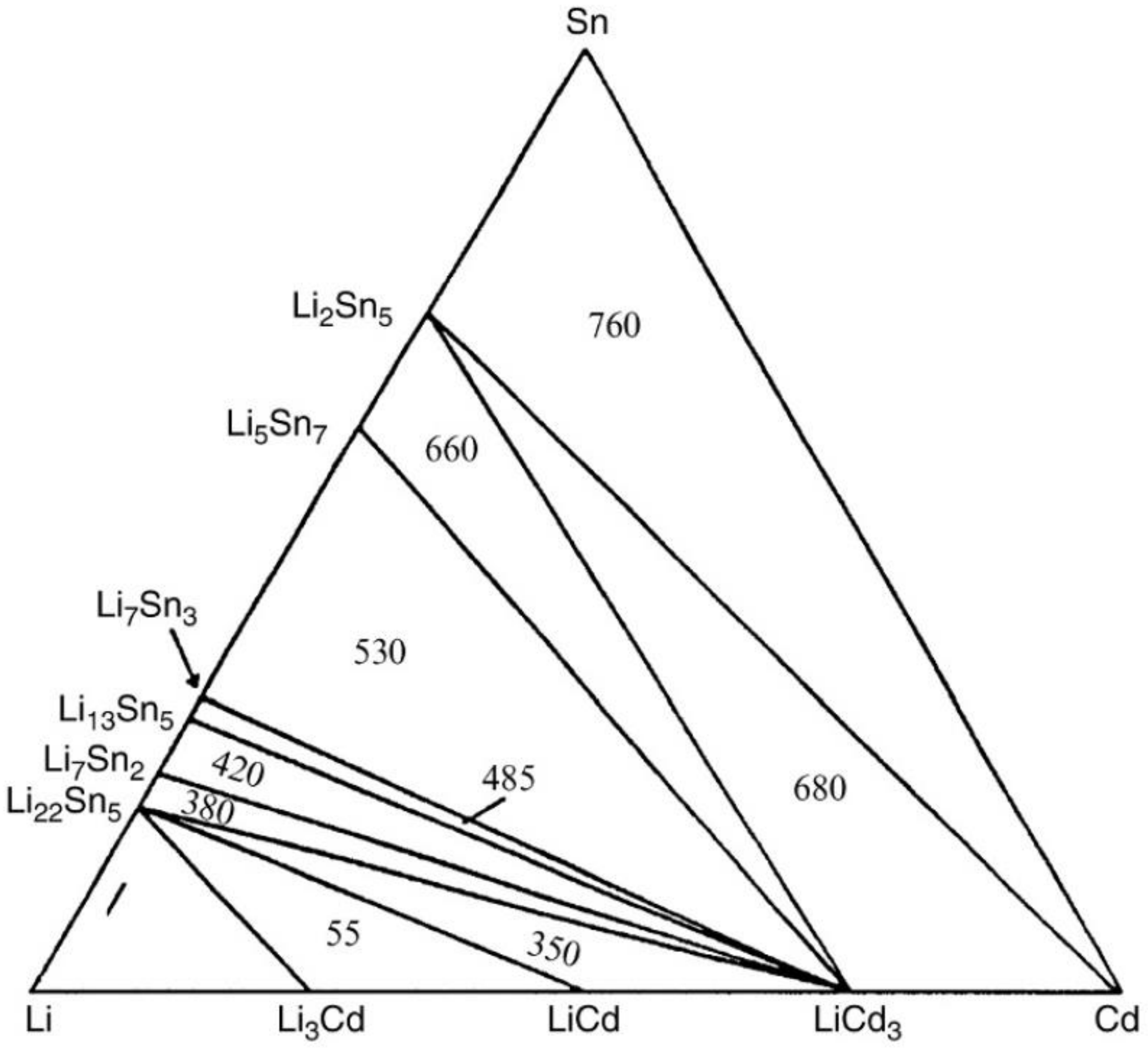

Fig. 7B.5 Calculated phase stability diagram for the Li–Cd–Sn system at ambient temperature. Numbers are voltages (millivolts) vs. Li phase $Li_{4.4}Sn$, which has fast chemical diffusion for lithium, is stable at the potentials of two of the Li–Cd reconstitution reaction plateaus, and therefore can be used as a matrix phase. The behavior of this composite electrode, in which Li reacts with the Cd phases inside of the Li–Sn phase

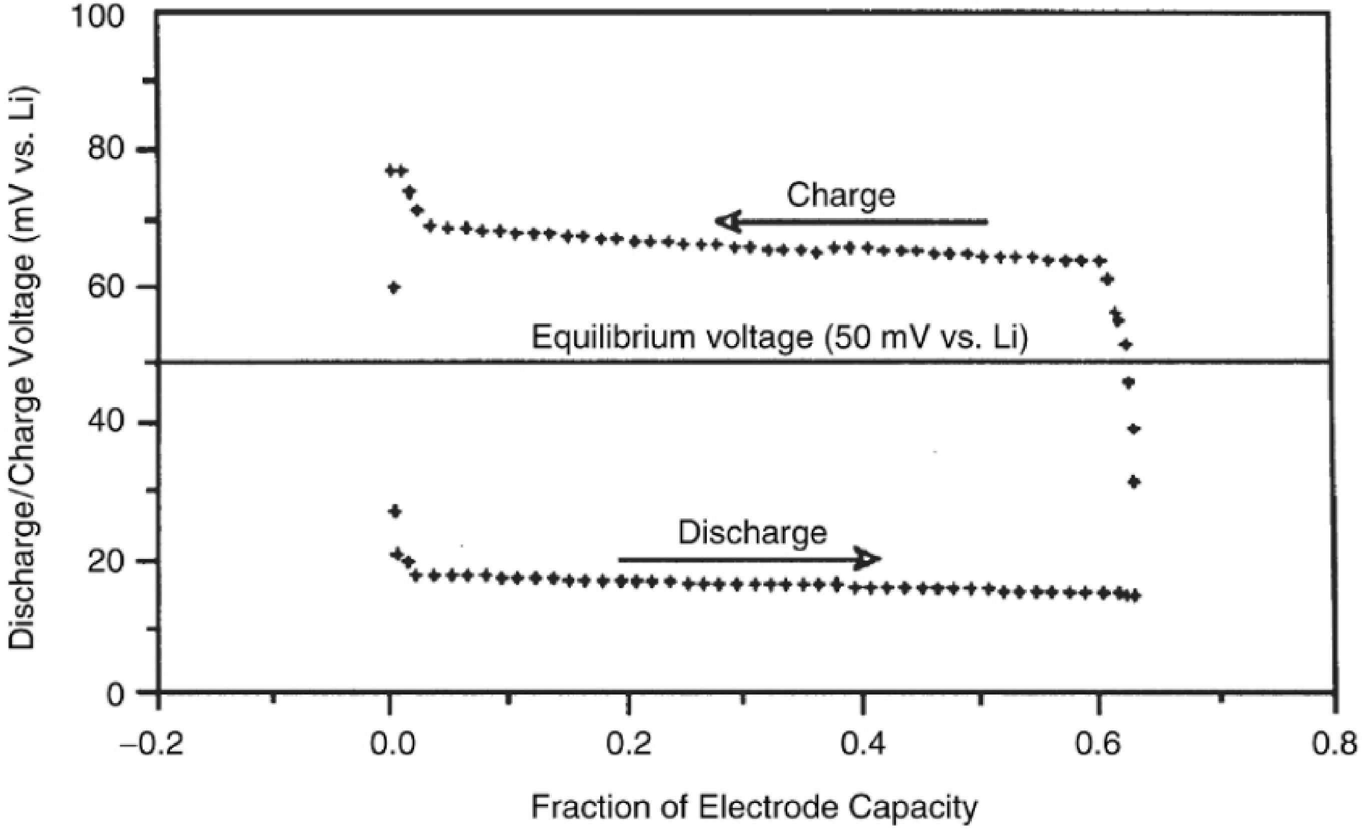

Fig. 7B.6 Charge–discharge curve of the Li–Cd system with a fast mixed-conducting phase in the lithium–tin system at ambient temperature

(4) Decrepitation (파열)

-volume changes upon the insertion of guest → decrepitation or crumbling(부스러짐) → result in the loss of electronic contact between reactive constituents in the microstructure and the current collector → the reversible capacity decreases

-Li-Sn system: highest lithium concentration, $Li_{4.4}Sn$ → specific volume 283% of pure Sn

-Electrochemical cycling behavior is significantly improved if the initial particle size is already very small, and it is reasonable to conclude that this is related to the terminal particle size phenomenon → modeling of particle size (Fig. 7B.7)

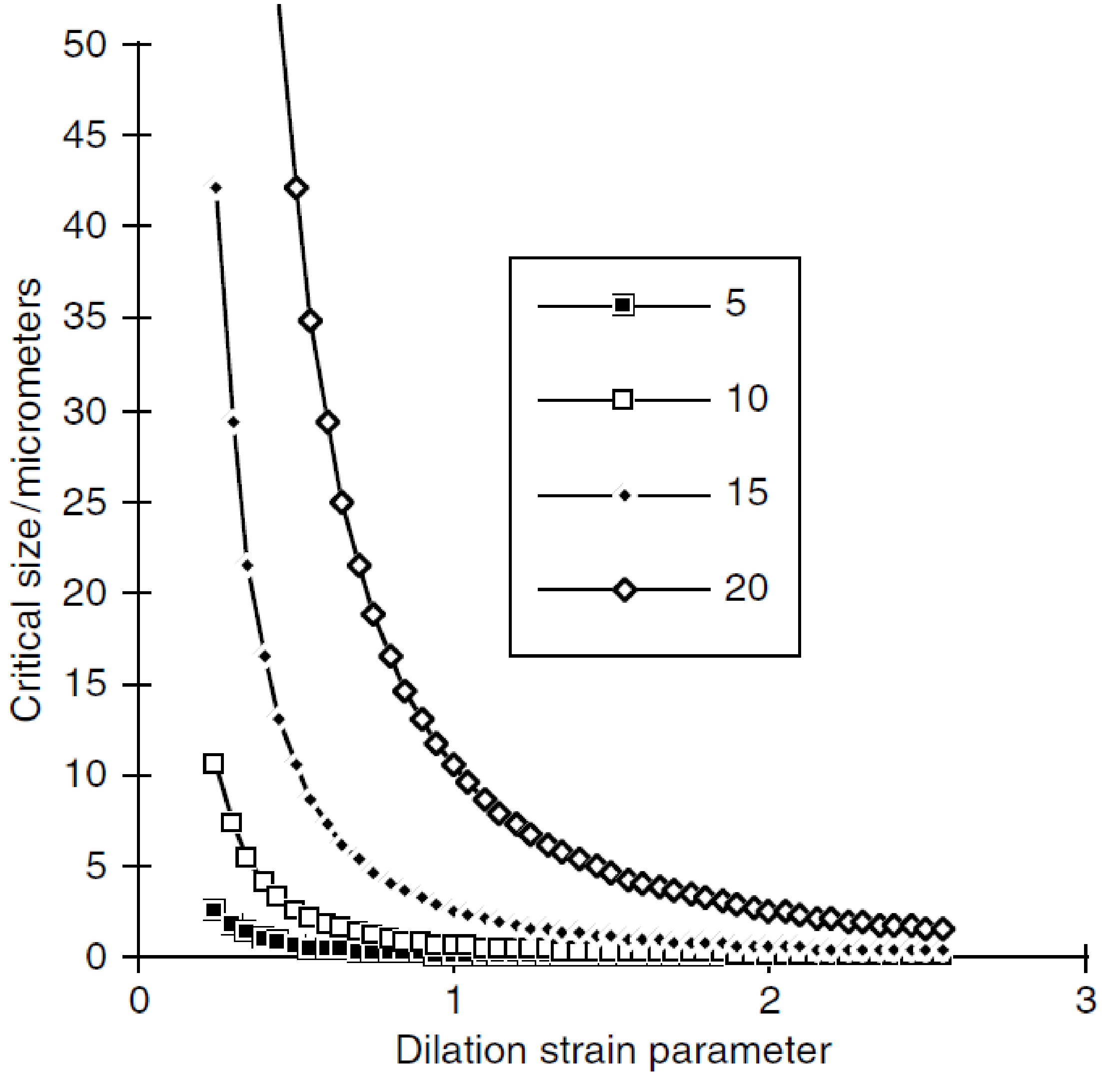

Fig. 7B.7 Variation of the critical particle size as a function of the dilation strain for several values of the fracture toughness of the phase in tension

-volume change depends upon the amount of lithium that has entered the alloy crystal structure, and is essentially the same for all lithium alloys

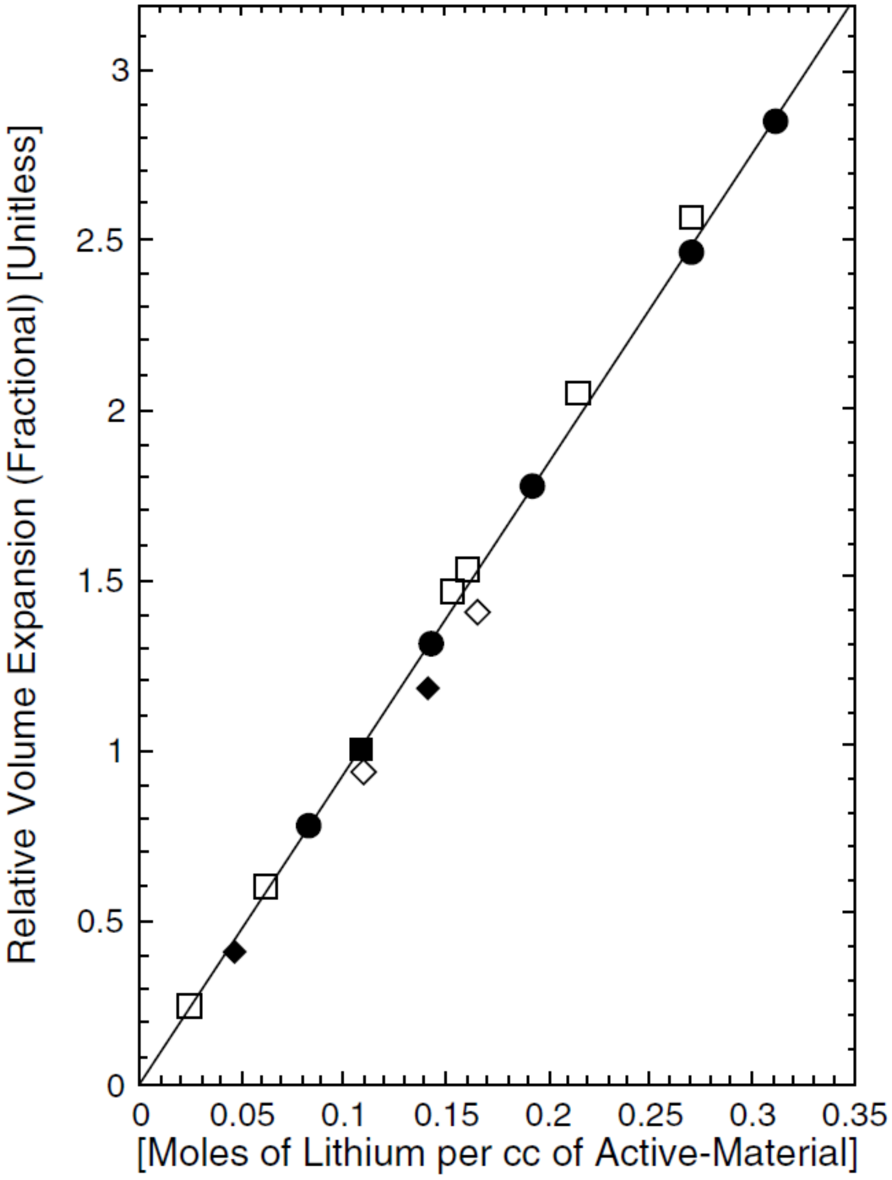

Fig. 7B.8 Relation between volume expansion and the amount of lithium introduced into lithium alloys

(5) Modification of the Micro and Nanostructure of the Electrode

-some innovative of large volume changes inherent in the use of metal alloy and silicon negative electrodes in lithium systems

room to breathe + maintaining electric contact with current collector

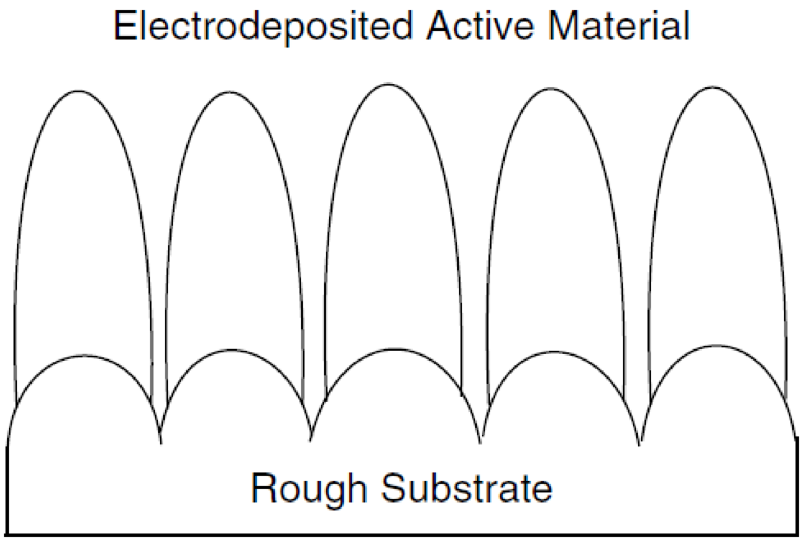

Fig. 7B.9 Schematic drawing of the preferential deposition of reactant material upon protrusions on the substrate surface

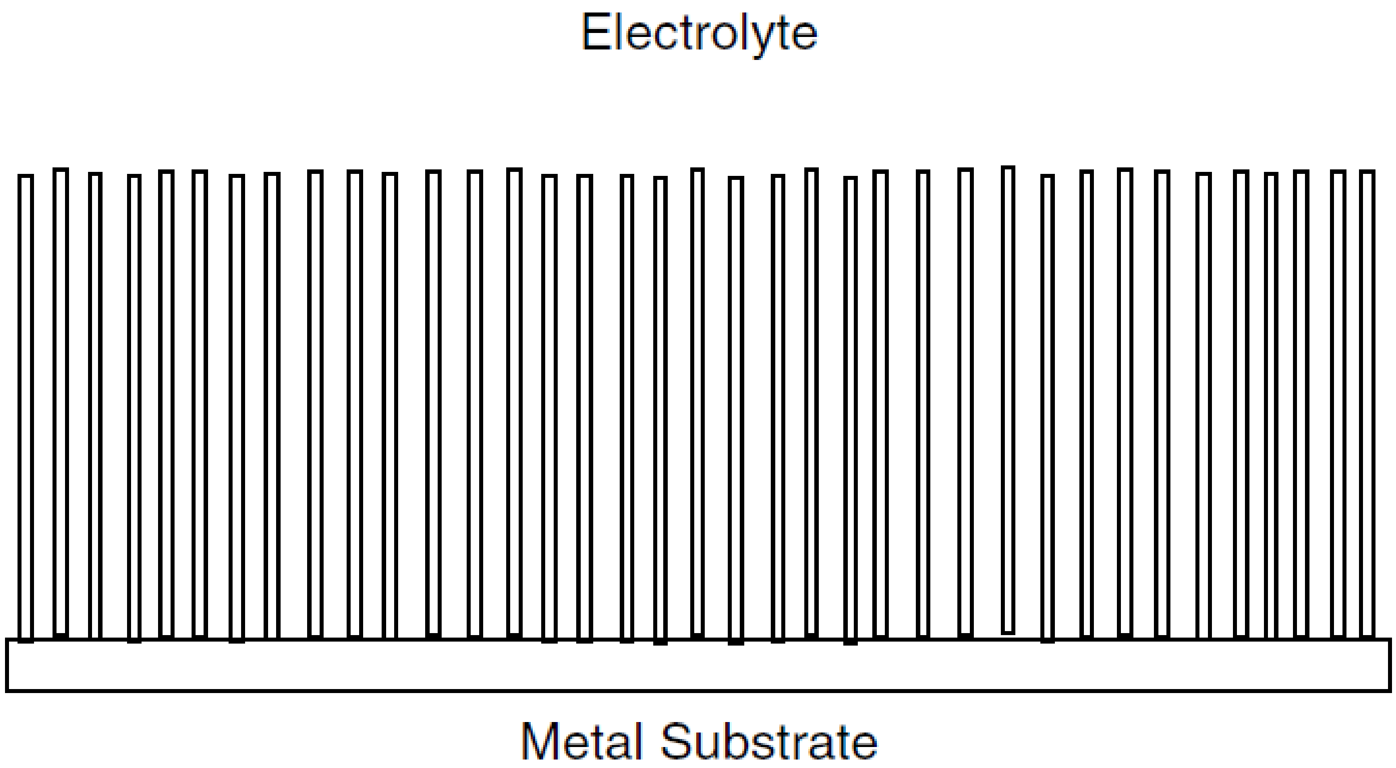

Fig. 7B.10 Schematic drawing of electrode with a large number of nanowires